Journal of Applied Polymer Science

Electronic Properties of Polypyrrole Based TiO_2 Nanofiber Composite

Dinesh Chandra Tiwari,[1] Priyanka Atri,[1] Rishi Sharma[2]
[1]SOS Physics, Jiwaji University, Gwalior 474011, India
[2]CSIR-CEERI, Pilani 333031, India
Correspondence to: D. C. Tiwari (E-mail: dctiwari2001@yahoo.com)

ABSTRACT: In this work, Polypyrrole (PPy), Titanium dioxide nanofiber (TiO_2-nf) are prepared by oxidative polymerization and hydrothermal process respectively. The PPy/TiO_2-nf composite is prepared by *in situ* oxidative polymerization in the presence of pyrrole monomer and TiO_2-nf. The nanocomposite and TiO_2-nf are then characterized by scanning electron microscopy (SEM) and energy dispersive X-ray spectroscopy (EDX) techniques and XRD studies. Dielectric studies of PPy/TiO_2-nf composite is carried out in the frequency range of 1 KHz-3 MHz at varying temperature and it shows anomalous behavior at 1MHz, where its value reaches to its minimum value of 13 at room temperature and this dip remains even at higher temperature. Impedance study is used to understand the grain and grain boundary effects of the material; frequency dependent ac conductivity has two regions separated at 1MHz, which is being explained by hopping conduction and Maxwell-Wagner type mechanism, respectively. © 2013 Wiley Periodicals, Inc. J. Appl. Polym. Sci. **2014**, *131*, 40036.

KEYWORDS: nanoparticles; nanowires and nanocrystals; dielectric properties; composites; conducting polymers

Received 25 June 2013; accepted 4 October 2013
DOI: 10.1002/app.40036

INTRODUCTION

Nanomaterials exhibit quantization effects due to confinement of electrons, this leads to the introduction of discrete energy levels, which produces different properties as compared to the bulk material, and they are more attractive due to high surface area to volume ratio.[1,2] The properties of nanocomposite films depend not only upon the individual components used but also on the morphology and the interfacial characteristics. Anatase TiO_2 is very promising material and has many applications in different field such as in photocatylysis,[3,4] dielectric ceramics, solar cell, sensors, biomedical, optoelectronic, and microelectronics devices.[5–8]

Polypyrrole (PPy) is a p-type conducting polymer and have attracted great interest due to its high conductivity and environmental stability. Recently various attempts have been made to incorporate TiO_2 nanoparticles in conducting polymers such as polyaniline (PANI),[9] poly (phenylenevinylene) (PPV),[10] and poly (methylmethacrylate) (PMMA)[11] with the aim of obtaining high conductivity and high dielectric constant. A giant dielectric constant of titania-PPy nanocomposite was reported by Dey et al.[12] they have studied the impedance and dielectric properties as a function of frequency and temperature at different compositions. The high dielectric constant in the composite was due to interfacial polarization. Kontos et al.[13] have studied the electrical relaxation dynamics in TiO_2–polymer matrix with different composition. In this study, they found the two relaxation modes namely β and γ in low temperature region. Wei et al.[14] reported the fabrication and characterization of mesoporous TiO_2/PPy based nanocomposite for electrorheological (ER) fluid. It was found that PPy doped TiO_2 (ER) fluid has larger value of dielectric constant in the frequency range from 10^2 to 10^5 Hz.

Dielectric spectroscopy and AC conductivity studies of PPy/TiO_2 nanocomposite were reported by Kumar and Sarmah[15] they found that the dielectric constant decreases with increase in frequency. The dielectric relaxation time was found to decrease with the increase in TiO_2 concentration. Wei et al.[16] measured the frequency dependent dielectric constant of PPy/TiO_2 nanocomposite prepared by different oxidant in the frequency range from 20 Hz to 2 MHz. It was found that the significant increase in dielectric constant was due to Maxwell-Wagner-Sillers effect for the nanocomposite oxidized by $FeCl_3$. TiO_2 nanostructures such as nanotubes, nanorods and nanowires have recently attracted attention due to its unique properties; quantum confinement, small size and defects in grains are few factors responsible for different properties of nanostructured TiO_2.[17] We have successfully prepared composite of PPy/TiO_2-nf, the presence of inorganic materials strongly affect the properties of the polymers.

We have summarized the work reported by other authors on PPy–titanium dioxide nanocomposite. The results obtained by

us clearly indicate the anomalous dielectric behavior of this composite. We have explained the result by using two different conductivity mechanisms below and above the 1 MHz.

In this article, we report our work on PPy/TiO_2-nf composites, synthesized by the oxidative polymerization of pyrrole in the presence of TiO_2-nf. The PPy and its composite are characterized by scanning electron microscopy (SEM) and EDX analysis. Dielectric properties, impendence spectroscopy and ac conductivity are also measured at varying temperature to understand the charge transport mechanism. Dielectric properties of PPy/TiO_2–nf are showing anomalous behavior at around 1 MHz, based on above literatures and also to the best of our knowledge; no report is available to date in the literature about such behavior of PPy/TiO_2-nf nanocomposite.

EXPERIMENTAL

Preparation of TiO_2-nf

TiO_2-nf was prepared by using hydrothermal method. TiO_2 [Riedel-de Hain make] was suspended in 10*M* NaOH (Merck) solution and heated at 100°C for 3 h with constant stirring using magnetic stirrer. The pH of the suspension was maintained at 5 by adding 1*M* HCl (Merck) with continuous stirring for 5 h, so that complete ion exchange reaction takes place. The sodium ion was completely removed with the formation of Na^+ and Cl^- ions. The solution was allowed to stay for 8 h and allowed to settle down the suspended TiO_2-nf nanoparticles. After the process, the solid material was filtered off and washed with double distilled water, and dried at 100°C. TiO_2-nf was characterized by SEM and XRD.

Preparation of PPy/TiO_2-nf Composite

The synthesized TiO_2-nf was dispersed in 6 wt % solution of $FeCl_3$ (Merck), this mixture was heated upto 80°C with constant stirring for 2 h and reaction mixture was allowed to cool. Pyrrole (Aldrich) monomer (99%) was purified under reduced pressure and solution of 0.1*M* pyrrole was added drop-wise to TiO_2-nf-$FeCl_3$ mixture with constant stirring and the resultant solution mixture was stirred continuously at room temperature for 2 h. The resulting precipitate was collected and washed repeatedly with methanol and double distilled water to remove the oxidant. Finally, the sample was dried under vacuum at 30°C for 24 h. All the chemicals and reagents used in experiments are of analytical grade.

RESULT AND DISCUSSION

Morphology and the elemental composition of TiO_2-nf and PPy/TiO_2-nf composite are characterized by SEM and EDAX, respectively. Figure 1(a–c) shows the SEM image of TiO_2-nf, PPy, and PPy/TiO_2-nf composite, respectively. SEM image of TiO_2 nanofibers [Figure 1(a)] having diameter of approximately 30 nm, whereas Figure 1(b) shows the micrograph of PPy, which is cauliflower structure. SEM image of PPy/TiO_2 nanocomposite is shown in Figure 1(c), it indicates that the TiO_2-nf are encapsulated by the PPy and the grain size is in the range of nearly 70-90 nm. EDX analysis confirms the presence of TiO_2-nf

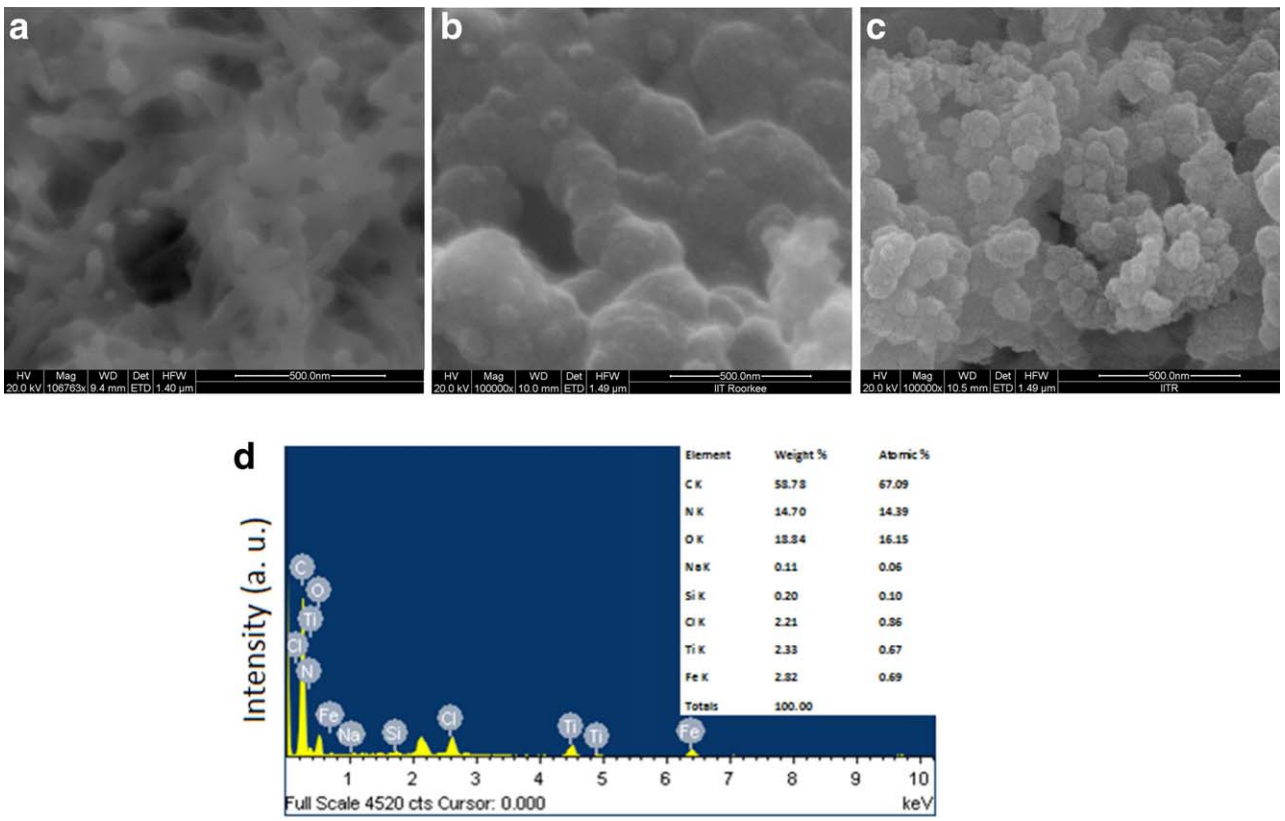

Figure 1. (a) SEM image of TiO_2-nf, (b) SEM image of chemicaly synthezised PPy, (c) SEM image of PPy/TiO_2-nf composite, (d) EDX analysis of the PPy/TiO_2-nf composite. [Color figure can be viewed in the online issue, which is available at wileyonlinelibrary.com.]

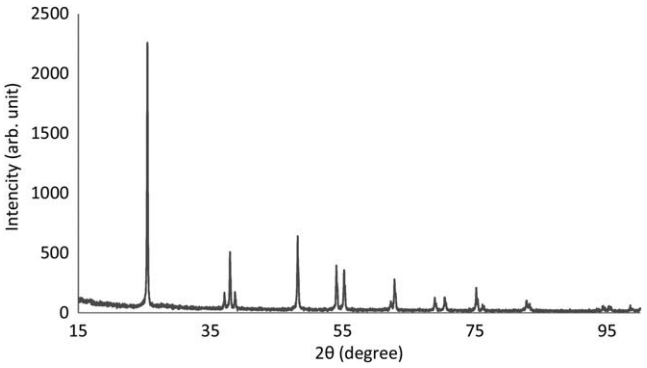

Figure 2. XRD analysis of TiO_2-nf.

[Figure 1(d)] a core–shell structure is visible and core is made up of TiO_2. TiO_2-nf was also characterized by XRD, Figure 2 shows the XRD peaks which confirm the anatase phase in TiO_2-nf and the peaks are matching with that of JCPDS, card no. 21–1272, crystallite size was found to be nearly 31 nm calculated by using Scherrer formula. For electrical measurements, pellets of diameter 0.949 cm and thickness 0.65mm were prepared by using hydraulic press. Dielectric constant and dissipation factor (tan δ) measurement in the frequency range 1 kHz to 3 MHz were carried out using a Hioki-3532 LCR Hi Tester at different temperatures (25–100°C).

Dielectric Measurement

The frequency-dependent dielectric constant and dielectric losses of pure PPy, TiO_2-nf and PPy/TiO_2-nf composites were measured from 1 KHz to 3 MHz frequencies at different temperature, i.e., 25°C, 50°C, 75°C, and 100°C, respectively. The dielectric constant was calculated by using capacitance (C), thickness of the pellet (d), the free space charge permittivity (ϵ_o) and the area of the capacitor plate (A) by following formula

$$\epsilon' = \frac{Cd}{\epsilon_o A} \tag{1}$$

$$\epsilon = \epsilon' - j\epsilon'' \tag{2}$$

$$\epsilon' = \frac{C}{C_o} \text{ and } \epsilon'' = \frac{1}{\omega R C_o} \tag{3}$$

Figure 3(a) shows the real part of permittivity of undoped PPy at different temperature, in the frequency range from 1 KHz to 3 MHz. The dielectric constant of PPy has been found to increase with increase in temperature from 25°C to 100°C and decreases with increasing frequency at all temperatures. Decreases in ϵ' of PPy [Figure 3(a)] with increase in frequency are due to the dielectric relaxation phenomenon. At low frequency dipoles follow the field and as frequency increases dipoles begin to lag with the field and hence ϵ' decreases.[18] Figure 3(b) shows the variation of TiO_2-nf with frequency at 25°C. Here a slight dip was observed at 1 MHz. Other than slight dip in dielectric constant around 1 MHz, the overall dielectric trends are similar to Figure 3(a). Presence of the dip in TiO_2-nf is due to dielectric relaxation. The value of ϵ' for TiO_2-nf varies from 60 to 34.3 in the entire frequency range at 25°C. The dip at 1 MHz is enhanced with incorporation of TiO_2-nf into PPy. Dielectric permittivity of a material depends on the polarizability of the molecules, higher the polarizability of the material, higher is the permittivity of the material. In case of nanocomposites having polymers and inorganic nanomaterial the orientation polarization and interfacial polarization plays an important role, interfacial polarization arises from the electrically heterogeneous materials where two phases differ from each other in dielectric constant.[19,20] At low frequency, the permanent dipoles align themselves along the field and contribute fully to the total polarization of the dielectric, whereas at higher frequency, the variation in the field is too rapid for the dipoles to align themselves, so their contribution to the polarization and, hence to the dielectric permittivity becomes negligible. Therefore, the dielectric permittivity ϵ' decreases with increasing frequency.[21]

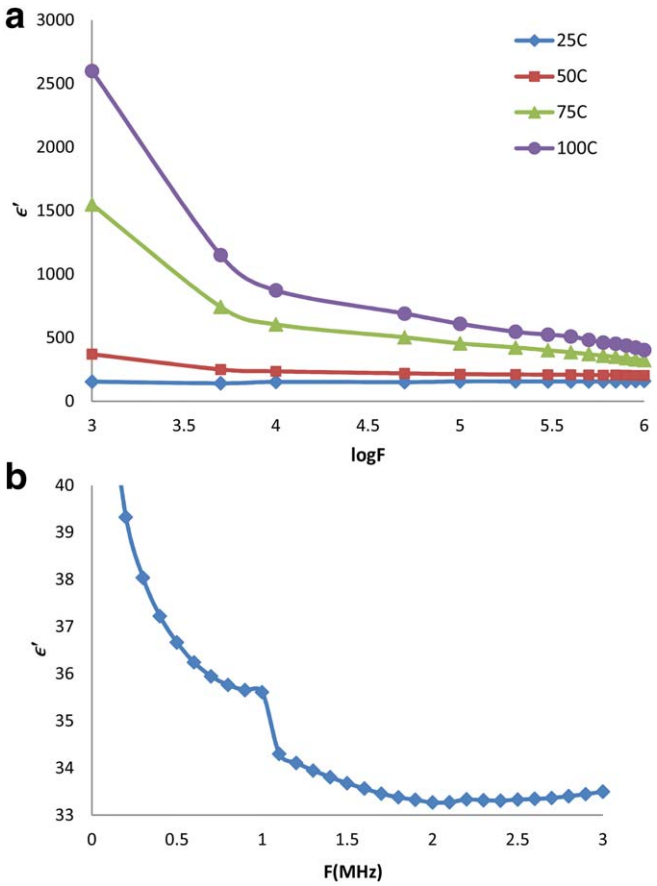

Figure 3. (a) Dielectric behavior of PPy with frequency, (b) Variation of dielectric constant of TiO_2-nf with frequency. [Color figure can be viewed in the online issue, which is available at wileyonlinelibrary.com.]

Frequency and temperature dependent ϵ' of PPy/TiO_2-nf composite is shown in Figure 4(a), ϵ' is strongly influenced by the presence of TiO_2-nf, and the value of ϵ' in case of PPy/TiO_2-nf increases to 14,000 (at 1 kHz and 100°C) [shown in inset of Figure 4(a)] from the corresponding value of ϵ' [see Figure 3(a)] to 2600 (at 1 kHz and 100°C). Overall large value of ϵ' is due to Maxwell-Wagner Sillars effect in which the charge carriers are accumulated at the interfaces of nanocomposite.[12,22] The SEM images of PPy/TiO_2-nf composite shows the incorporation of TiO_2-nf in PPy matrix. This shows that the value of ϵ' increases with formation of microcapacitors in the composite.

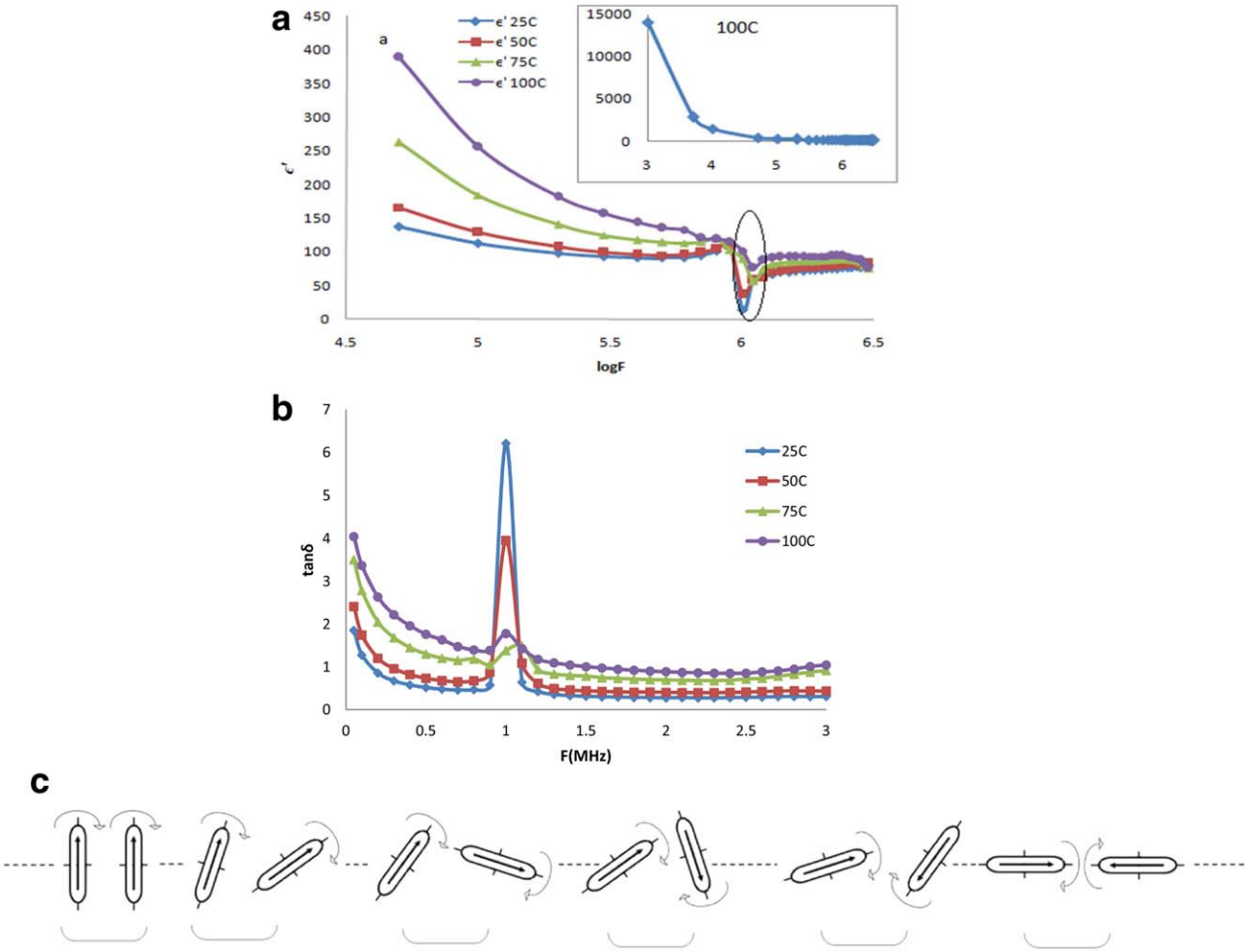

Figure 4. (a) Dielectric behavior of PPy/TiO_2-nf composite with frequency at various temperatures (inset shows the high dielectric constant of PPy/TiO_2-nf composite at 100 C), (b) Variation of tan δ of PPy/TiO_2-nf composite with frequency at different temperature, and (c) Orientation of dipoles in PPy/TiO_2-nf composite with changing frequency. [Color figure can be viewed in the online issue, which is available at wileyonlinelibrary.com.]

The dielectric measurement of PPy/TiO_2-nf composite reported here have anomalous behavior around 1 MHz frequency, this dip remains consistent even at elevated temperatures but slight shift of dip is observed [Figure 4(a)] which indicates the effect of temperature on relaxation phenomena. At 1 MHz, a sharp decrease in dielectric permittivity of PPy/TiO_2-nf composite is observed as shown in Figure 4(a), to the best of our knowledge, there are so far no reports for such type of sudden variation at 1 MHz. At this frequency the conductivity also increases with the free movement of the charges through the conducting path provided by TiO_2-nf in the matrix. As a result of this the variation of ϵ' at 1 MHz is also enhanced and we see a variation of $\Delta\epsilon' = 101.2$ at this frequency. In nanocomposite at varying frequency, the relaxation time of PPy and TiO_2-nf are different and will be out of phase at 1 MHz [Figure 4(c)]. We have done extensive studies on this material and presence of dip was found to be consistent. Figure 4(b) shows the dielectric loss curve for PPy/TiO_2-nf composite at different temperature (25°C to 100°C). The graph of dielectric loss with frequency shows a peak around 1 MHz due to completely constructed electron transport channel, indicating increased flow of charge carrier, hence the losses are also maximum at this frequency and it is also visible in the conductivity graph [Figure 6].

Impedance Analysis

Impedance measurement with respect to frequency is important to inspect the detailed physical processes occurring inside the materials through their electrical analogs.[23] The most important advantage of impedance measurements is that they can distinguish individual contributions to electrical conduction or to polarization from different sources, like the bulk, grain boundaries, intergranular contact regions, and electrode–sample interface regions where defects are generated.[24] Temperature dependent impedance spectroscopy is analyzed by considering equivalent circuit consisting of two parallel RC elements connected in series [Figure 5(b)]. This circuit is used very widely with materials whose properties are some combination of bulk, grain and grain boundary. Since the grain boundaries exhibit normally higher resistance than the grain interiors, the first semicircle in the high frequency region could be attributed to the behavior of grain interior while the second semicircle in the lower frequency region is attributed to the grain boundaries.

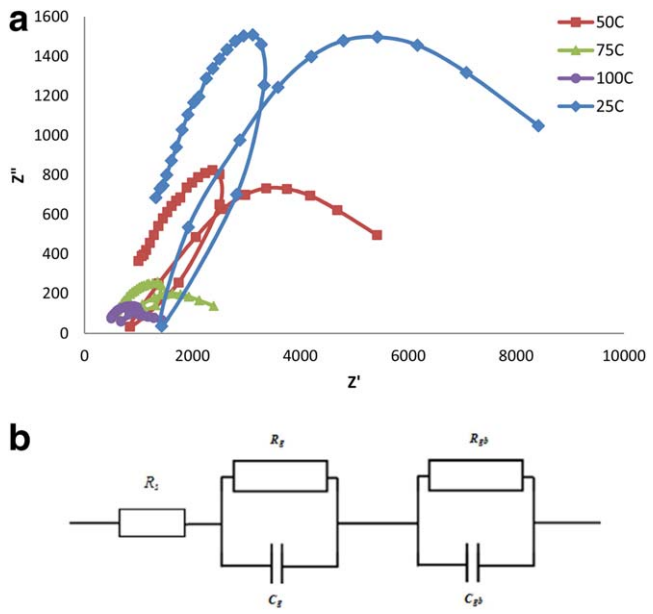

Figure 5. (a) Nyquist plot of PPy/TiO_2-nf composite at different temperature, (b) Equivalent circuit consisting of two parallel RC element connected in series with Rs. [Color figure can be viewed in the online issue, which is available at wileyonlinelibrary.com.]

The bulk and grain boundary effects are represented by the parallel R_g-C_g and R_{gb}-C_{gb}, combination, respectively.

The derivation of impedance (voltage/current) of circuit element is shown in eqs (4)–(8),

$$Z = Z' - iZ'' \tag{4}$$

$$Z\prime = R_s + \frac{1}{\frac{1}{R_g} + i\omega C_g} + \frac{1}{\frac{1}{R_{gb}} + i\omega C_{gb}} \tag{5}$$

$$Z'' = R_g\left[\frac{\omega R_g C_g}{1+(\omega R_g C_g)^2}\right] + R_{gb}\left[\frac{\omega R_{gb} C_{gb}}{1+(\omega R_{gb} C_{gb})^2}\right] \tag{6}$$

The intercepts of the these semicircles are used to calculate the resistance corresponding to grain (R_g) and grain boundary (R_{gb}),while the corresponding frequency values are evaluated from the apex of the semicircles and are used to calculate the capacitance corresponding to grain (C_g) and grain boundary (C_{gb}) from in following equations.

$$2\pi f_g C_g R_g = 1 \quad 2\pi f_{gb} C_{gb} R_{gb} = 1 \tag{7}$$

And relaxation time for grain (τ_g) and grain boundary (τ_{gb}) are given by following equation

$$\tau_g = R_g C_g \quad \tau_{gb} = R_{gb} C_{gb} \tag{8}$$

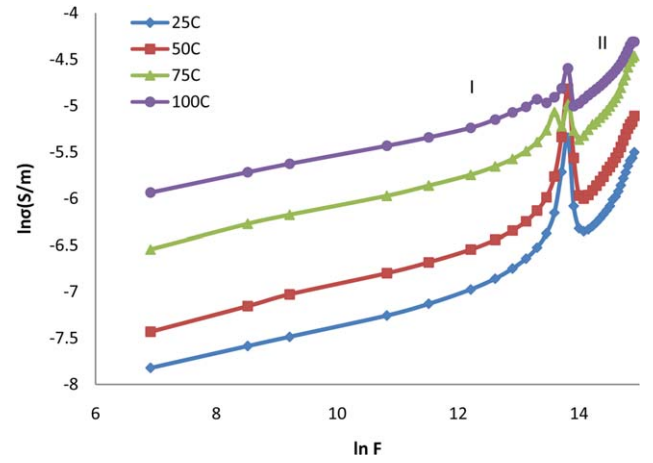

Figure 6. AC conductivity of PPy/TiO_2-nf composite with frequency at different temperatures. [Color figure can be viewed in the online issue, which is available at wileyonlinelibrary.com.]

As seen in Figure 5(a) that the complex impedance plots at different temperatures do not coincide with the origin and hence there is a series resistance R_s connected to the circuit.[25,26] The relaxation frequency of PPy/TiO_2-nf composite for grain and grain boundary is studied by Nyquist plot [Figure 5(a)], and usually its response is in semicircular form.[27] The centre of the semicircular arc's shifts toward the origin on increasing temperature as well as frequency which indicates that the a.c. conductivity of the samples increases with increase in temperature,[28] and this behavior is also observed in Figure 6. The appearance of two arc's (one is for the grain boundaries at higher frequency region and second arc at low frequency is due to the grain effect) at all temperature [Figure 5(a)], which means that the electrical process obey two different relaxation mechanisms associated with grain and grain boundary. It is also to be noted that the crossover region occurs at the nearby 1 MHz frequency, indicating a sudden dip in Figure 4(a) is associated with the grain and grain boundary effects. The two semicircles at high and low frequencies can be assigned to charge transport mechanism within the grain interior and grain boundary effect. Initially when temperature is 25°C, both semicircle for bulk grain and grain boundary are equally dominant [Figure 5(a)]. At high temperatures, the grain interior semicircle is more dominant in comparison to the grain boundary and this behavior goes on increasing with rise in temperature, due to this effect dielectric constant increases with increasing temperature as seen in Figure 4(a).

AC Conductivity

Electrical conductivity with varying frequency and temperature is shown in Figure 6, usually ac conductivity increases with the increase in frequency, and also increases with increase in temperature. The conductivity increases with increase in temperature is due to the thermally activated conduction hopping process. Conduction in materials is usually divided into two classes, band conduction and dc hopping conduction, the band conduction exists in the absence of defects and impurities, and it is led by the band structure of the material, whereas dc hopping conduction, takes place via defects or impurities which forms potential wells (traps or localized states) that are favorable for charge carriers (electrons, holes, and ions) to hop.[29] It has been observed that the electrical conductivity of dielectric material containing polymer nanocomposite may be expressed as the sum of frequency independent conductivity $\sigma(0)$ and frequency-dependent component of conductivity $\sigma(\omega)$, ω is angular frequency, s is dimensionless parameter in the range $0 << s << 1$ and β is a constant, and are shown as

$$\sigma_{ac} = \sigma(0) + \sigma(\omega) = \beta\omega^s \tag{9}$$

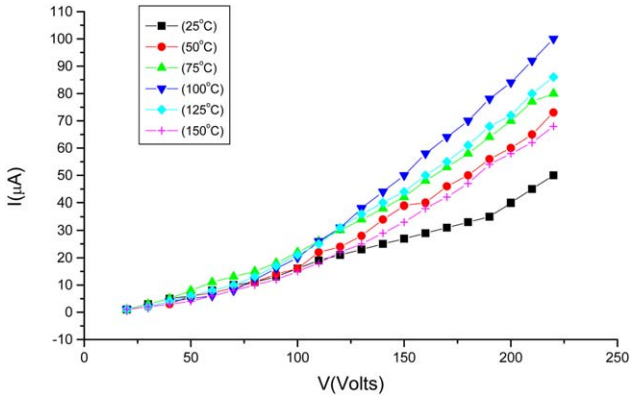

Figure 7. I-V characteristic of TiO_2-nf with temperature. [Color figure can be viewed in the online issue, which is available at wileyonlinelibrary.com.]

$$s = \frac{d\ ln\sigma(\omega)}{d\ ln\omega} \tag{10}$$

The frequency exponent "*s*" is shown in eq. (9) and can be calculated from the slope of the plot $ln\sigma(\omega)$ and $ln\omega$. The AC conductivity of pure PPy is 2.81×10^{-2} S/m at 25°C, whereas for PPy/TiO_2-nf it decreases to 4.0×10^{-4} S/m at 25°C, there is overall decrease in conductivity in a nanocomposite formed by incorporation of TiO_2-nf into PPy (Figure 6). Conductivity changes at the sites where the bonds between a polymer chain and nanofiber are formed, the electronic configuration in the polymer chain changes, s-p hybridization occurs and the overlapping of π orbitals diminishes, the conjugation length therefore decreases, causing the corresponding increase in band gap, and hence effects the conductivity,[30,31] It is already explained above that the hopping conduction occurs in heterogeneous media, having both amorphous and crystalline phases, changes in ac conductivity is due to the accumulation of charges at the interface of grain and grain boundary and the formation of large dipoles on metal particles or cluster.[32,33]

The conductivity increases with frequency and a peak is observed at a frequency of about 1 MHz, this is close to the frequency at which the dielectric constant shows a sudden dip. To explain the AC conductivity in PPy/TiO_2-nf composite, ac conductivity is divided into two regions, region-I (1 kHz to 1 MHz frequency) and region II (1 MHz onward). In region-I value of $S < 1$ (Figure 6), conductivity increases linearly with frequency, at frequency around 1 MHz a sudden peak appears, and then thereafter conductivity increases monotonically. It is to be noted that at 1 MHz, on increasing the temperature the discontinuity have a decreasing trend. The appearance of sudden peak at 1 MHz indicates that some form of polarization becomes active.

Region II in Figure 6, the value of frequency exponent s >1 i.e of the order of 1.01. Hence the results are difficult to explain on the basis of hopping conduction. In the heterogeneous composite consisting of amorphous and nanofibers (crystalline), will have regions of differing electrical conductivity which must give rise to frequency dispersion corresponding to Maxwell-Wagner type.[31–34] This region II also corresponds to interfacial relaxation. The origin of interfacial relaxation is related to the existence of free charge carriers inside the system. The charges can migrate under the influence of applied electric field accumulating at the interfaces between the media with significantly different conductivity and permittivity.

I-V characteristic of the TiO_2-nf is plotted in Figure 7. It is found that initially the current increases with increase in temperature upto 100°C, and thereafter on further increase of temperature the current reduces. This shows that the sample is becoming insulator. It is also visible in ac conductivity, on increasing temperature there is increase in conductivity as seen in (Figure 6). It has been found by several experiments that Ti^{3+} state is formed at the surface of TiO_2 nanofibers.[35,36] Thus the formation of Ti^{3+} distorts the octahedral of TiO_6. The experimental and theoretical results indicate that the co-ordination of Ti surface atom reduces from six co-ordinates to five co-ordinates,[37,38] thus the octahedra get distorted. The occurrence of dip in Figure 4(a) is attributed to the change of oxidation state of the Ti, as it is known that the conductivity of Ti^{3+} is higher than Ti^{4+}, and it is also reported that the process is reversible. Occurrence of such peak is affected by many factors hence it is difficult to predict any one of them. Switching phenomena in PPy and TiO_2 are reported where they are oxidized and reduced as per the polarity of applied bias[39] and the enhancement in the peak is also affected by the encapsulation of PPy into TiO_2-nf. Conducting polymer passivates the surface of TiO_2 nanofibers electronically. The large difference in polarization properties between TiO_2 and PPy modifies the energy levels of PPy in the vicinity of nanofibers.[31] Thus the charge transport process of polymers is influenced by TiO_2.

CONCLUSION

This study indicates a remarkable increase in dielectric constant of PPy/TiO_2-nf composite, the increase in dielectric constant is attributed to the Maxwell-Wagner Sillars effect. Temperature dependence impedance spectroscopy behavior of PPy/TiO_2-nf composite exhibits two semicircles, which indicate a distinct conduction phenomenon, occurs at grain and grain boundary. Presence of dip at 1 MHz is due to the frequency-dependent polarization and changing of oxidation state of Ti from Ti^{4+} to Ti^{3+} is also responsible for its occurrence. AC conductivity study shows two type of conduction mechanism in PPy/TiO_2-nf composite, hopping mechanism corresponds to $s < 1$ at low frequency region, and at higher frequency, the value of $s > 1$ and the conduction phenomena in this case is explained by Maxwell-Wagner effect.

REFERENCES

1. Harrison, P. Quantum Wells, Wire and Dots: Theoretical and Computational Physics of Semiconductor Nanostructure; Wiley, England, **2005**; Chapter *8*, p 243.
2. Gangopadhyay, R.; De, A. *Chem. Mater.* **2000**, *12*, 608.
3. Nakata, K.; Fujishima, A. *J. Photochem Photobiol C: Photochem Rev.* **2012**, *13*, 169.
4. Wu, H. B.; Hng, H. H.; Lou, X. W. *(D.). Adv. Mater.* **2012**, *24*, 2567.

5. Hua, Z. L.; Shi, J. L.; Zhang, L. X.; Ruan, M. L.; Yan, J. N. *Adv. Mater.* **2002**, *14*, 830.
6. Rothschild, A.; Komem, Y.; Levakov, A.; Ashkenasy N.; Shapira Y. *Appl. Phys. Lett.* **2003**, *82*, 574.
7. Lin, Y. P.; Lin, S. Y.; Lee, Y. C.; Chen-Yang, Y. W. *J. Mater. Chem. A*, in press.
8. Li, Q.; Cheng, K.; Weng, W.; Du. P.; Han, G. *J. Mater. Chem.* **2012**, *22*, 9019.
9. Somani, P. R.; Marimuthu, R.; Mulik, U. P.; Sainkar, S. R.; Amalnekar, D. P. *Synth. Met.* **1999**, *106*, 45.
10. Zhang, J.; Ju, X.; Wang, B.; Li, Q.; Liu, T.; Hu, T. *Synth. Met.* **2001**,*118*, 181.
11. Elim, H.; Ji, W.; Yuyono, A. H.; Xue, J. M.; Wang, *J. Appl. Phys. Lett.* **2003**, *82*, 2691.
12. Dey, A.; De, S.; De, A; De, S. K. *J. Nanosci and Nanotech.* **2006**, *6*, 1427.
13. Kontos, G. A.; Soulintzis, A. L.; Karahaliou, P. K.; Psarras, G. C.; Georga, S. N.; Krontiras, C. A.; Pisanias, M. N. *eXPESS Polym. Lett.* **2007**, *1*, 781.
14. Wei, C.; Zhu,Y.; Jin,Y.; Yang, X.; Li, C. *Mater. Res. Bull.*, **2008**, *43*, 3263.
15. Kumar, A.; Sarmah, S. *Phys. Stat. Soli. A*, **2011**, *208*, 2203.
16. Wei, S.; Mavinakuli, P.; Wang, Q.; Chen, D.; Asapu, R.; Mao, Y.; Haldolaarachchige, N.; Young, D. P.; Guo, Z. *J. Electrochem. Society*, **2011**, *158*, K205.
17. Asiaha, M. N.; Mamat, M. H.; Khusaimi, Z., Abdullaha, S.; Rusopa, M. *IEEE Symp Business, Eng Ind Appl*, **2012**, 50.
18. Himanshu, A. K.; Choudhary, B. K.; Gupta D. C.; Bandyopadhayay, S. K.; Sinha, T. P. *Phys B.* **2012**, *405*,1608.
19. Tiwari, D. C.; Sen, V.; Sharma, R. *Ind. J. Pure Appl. Phys.* **2012**, *50*, 49.
20. Sen, S. E.; Yerli, Y.; Okutan, M.; Yilmaz, F.; Gunaydin, O.; Humes, Y.; *Mater. Sci. Eng. B*, **2007**, *138*, 284.
21. Dutta, A.; Sinha, T. P.; Shannigrahi, S. *Phys. Rev. B.* **2007**, *76*, 155113.
22. Tamura, R.; Lim, E.; Manaka, T.; Iwamoto, M. *J. Appl. Phys.* **2006**, *100*, 114515.
23. Hirose, N.; West, A. R. *J. Am. Ceram. Soc.* **1996**, *79*, 1633.
24. Pan, L. K.; Huang, H. T.; Sun, C. Q. *J. Appl. Phys.* **2003**, *94*, 2695.
25. Bo, Z.; Qing, Z.; Chang, A.; Yao J.; Zhao P.; Gunan F.; Wenwen K., *J Alloys Compounds*, **2012**, *512*, 132.
26. Prasad, K. D.; Kumari, L. K.; Chandra, K. P.; Yadav, K. L.; Sen, S. *Appl. Phys. A*, **2007**, *88*, 377.
27. Orton, J. W.; Powell, M. *J. Rep. Prog. Phys.***1980**, *43*, 1263.
28. Sahoo, P. S.; Panigrahi, A.; Patri, S. K.; Choudhary, R. N. P. *Bull. Mater. Sci.* **2010**, *33*, 129.
29. Tuncer, E.; Serdyuk, Y. V.; Gubanski, S. M. *IEEE Trans. Dielect. Elect. Insul.*, **2002**, *9*, 809.
30. Skotheim, T. A.; Elsenbaumer, R. L.; Reynolds, J. R.; Handbook of Conducting Polymer; Mercel Dekker, **1998**.
31. Musikhin, S.; Bakueva, L.; Sargent, E. H.; Shik, A. *J Appl. Phys.* **2002**, *91*, 6679.
32. Kamalasanan, M. N.; Kumar, N. D.; Chandra, S. *J. Appl. Phys.* **1993**, *74*, 679.
33. Tsangaris, G. M.; Psarras, G. C. *J. Mater. Sci.* **1999**, *34*, 2151.
34. Kitao, M. *Jpn J. Appl. Phys.***1972**, *11*, 1472.
35. Sanjinés, R.; Tang, H.; Berger, H.; Gozzo, F.; Margaritondo, G.; Lévy, F. *J. Appl. Phys.* **1994**, *75*, 2945.
36. Lu, X.; Wang, G.; Zhai, T.; Yu, M.; Gan, J.; Tong, Y.; Li, Y. *Nano Lett.* **2012**, *12*, 1690−1696.
37. Rajh, T.; Nedeljkovic, J. M.; Chen, L. X.; Poluektov, O.; Thurnauer, M. C. *J. Phys. Chem. B.* **1999**, *103*, 3515.
38. Rajh, T.; Chen, L. X.; Lukas, K.; Liu, T.; Thurnauer, M.C.; Tiede, D. M. *J. Phys. Chem. B.* **2002**, *106*, 10543.
39. Barman, S. Deng, F.; *McCreery, R. L. J Am. Chem. Soc.* **2008**, *130*, 11073.